JACS
JOURNAL OF THE AMERICAN CHEMICAL SOCIETY
Communication
pubs.acs.org/JACS

Covalently Bound Clusters of Alpha-Substituted PDI—Rival Electron Acceptors to Fullerene for Organic Solar Cells

Qinghe Wu,[†,∥] Donglin Zhao,[†,∥] Alexander M. Schneider,[†] Wei Chen,[‡,§] and Luping Yu*[,†]

[†]Department of Chemistry and The James Franck Institute, The University of Chicago, 929 E 57th Street, Chicago, Illinois 60637, United States

[‡]Materials Science Division, Argonne National Laboratory, 9700 Cass Avenue, Lemont, Illinois 60439, United States

[§]Institute for Molecular Engineering, The University of Chicago, 5747 South Ellis Avenue, Chicago, Illinois 60637, United States

Supporting Information

ABSTRACT: A cluster type of electron acceptor, TPB, bearing four α-perylenediimides (PDIs), was developed, in which the four PDIs form a cross-like molecular conformation while still partially conjugated with the BDT-Th core. The blend TPB:PTB7-Th films show favorable morphology and efficient charge dissociation. The inverted solar cells exhibited the highest PCE of 8.47% with the extraordinarily high J_{sc} values (>18 mA/cm^2), comparable with those of the corresponding $PC_{71}BM$/PTB7-Th-based solar cells.

We report the synthesis and characterization of a new electron acceptor based on covalently bound clusters of alpha-substituted PDI which rival fullerene for organic photovoltaic (OPV) solar cells with an efficiency >8.4%. The motivation of this work is to find a replacement for expensive fullerene derivatives as electron acceptors in OPV studies. Because the fullerene derivatives ($PC_{61}BM$, $PC_{71}BM$) have intrinsic drawbacks, including limited visible light absorption, high cost, and instability of morphology in the blend films,[1,2] the exploration of nonfullerene electron acceptors, which are readily tunable in chemical structure and synthetically accessible, is vital for the advancement of OPV field.[3]

Recently, several studies reported solution-cast nonfullerene BHJ solar cells showing the PCEs >8%, which indicate the potential of nonfullerene electron acceptors.[3c−e] A crucial issue is how to rationally design efficient nonfullerene electron acceptors.

Small electron-rich moiety coupled with multiple electron-deficient moieties (A_m-D-A_m) hold promise as high efficient acceptors for solar cells.[3i,4] The versatility of donor and acceptor structures makes the fine-tuning in optical, electronic, and film forming properties possible.[3b,f−h,5] Previous studies have shown that acceptors with twisted 3D structure improve the morphological compatibility with the donor polymers and lead to enhanced photovoltaic performance.[3a,b,6] Hence, highly twisted or nonfully conjugated donor moieties were used to build the acceptors with the nonplanar 3D geometry.[5a,7] However, the strongly twisted π-conjugation is likely to undermine the charge transport and diminish their potential as effective electron acceptors. We developed a highly efficient electron-acceptor TPB for solar cells (Scheme 1). The BDT-Th unit has a coplanar π-conjugated backbone, which is conjugated through at least three directions with each terminal. The α-substituted PDI derivatives are shown to exhibit superior photovoltaic performance over β-isomer because the α-position functionalized PDI shows better planarity which facilitates close packing of π-conjugated backbone.[8] We describe photovoltaic properties of solar cell devices based on TPB/PTB7-Th.

Scheme 1. Synthetic Route of TPB and Chemical Structure of PTB7-Th

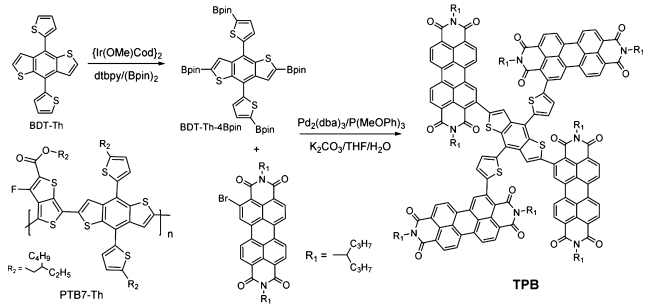

Synthesis. Selective borylation of BDT-Th via Ir-catalyzed reaction yields compound BDT-Th-4Bpin, which is purified by recrystallization in hexane. Suzuki coupling between BDT-Th-4Bpin with 4 equivalents of α-monobrominated PDI generates TPB. TPB exhibits high solubility in common organic solvents such as chlorobenzene and chloroform. The structure of TPB was characterized and confirmed by ^{1}H NMR, mass spectrum, and elemental analysis.

OPV Properties. Inverted solar cell devices were fabricated with the configuration of ITO/ZnO/TPB:PTB7-Th/MoO_3/Ag. The active layer with thickness of ~80 nm was deposited by spin-casting from hot chlorobenzene. The solar cell devices were tested under a simulated solar illumination of 100 mW/cm^2 AM 1.5G under nitrogen atmosphere. Table 1 summarizes the photovoltaic properties of the solar cells. The $J-V$ curves and EQE spectra are shown in the Figure 1.

Devices with varying TPB/PTB7-Th mass ratio from 1.5:1 to 1:1.5 were prepared and tested. The solar cells with 1:1 blend ratio show optimized average power conversion efficiency (PCE) of 6.62% with J_{sc} of 17.6 mA cm^{-2}, V_{oc} of 0.8 V, and FF of 0.47. Additives such as 1,8-diodooctane (DIO), dimethyl sulfoxide

Received: April 6, 2016
Published: May 24, 2016

DOI: 10.1021/jacs.6b03562
J. Am. Chem. Soc. 2016, 138, 7248−7251

Table 1. *J*–*V* Characteristics of Solar Cell Devices with TPB:PTB7-Th Active Layer

DPE (%)	J_{sc} (mA cm^{-2})	V_{oc} (V)	FF	Eff$_{ave}$ (%)[a]	Eff$_{max}$ (%)
0	17.6 ± 0.2	0.80 ± 0.00	0.47 ± 0.02	6.62 ± 0.33	7.03
5	15.6 ± 0.5	0.80 ± 0.00	0.58 ± 0.00	7.22 ± 0.22	7.62
8	17.9 ± 0.4	0.79 ± 0.00	0.58 ± 0.01	8.11 ± 0.26	8.47
10	16.1 ± 0.4	0.77 ± 0.01	0.54 ± 0.01	6.70 ± 0.20	6.90

[a]The PCEs were obtained from over 18 devices.

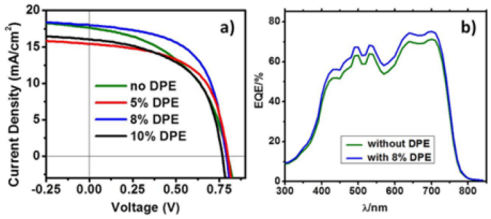

Figure 1. (a) *J*–*V* characteristics of TPB:PTB7-Th-based solar cell devices without/with 5%, 8%, and 10% DPE as additive. (b) External quantum efficiency spectra of TPB:PTB7-Th devices without/with 8% DPE as additive, which were sealed with Norland UV glue.

(DMSO), and diphenyl ether (DPE) are proved effective to further enhance the performance of devices. As shown in Table S1, addition of a small amount of DIO (0.12% v/v) or DMSO (0.15% v/v) can significantly improve the PCE from 6.62% to 7.34% and 7.44%, respectively. The PCE enhancement comes from the increase of FF from 0.47 to 0.53 and 0.54, respectively.

It was also found that the addition of 5% diphenylether (DPE) can improve the FF of device from 0.47 to 0.58; accompanied by slight decrease in the J_{sc} value. The highest PCE of 8.47% (average PCE of 8.11%) was achieved with 8% DPE. The high J_{sc} value (>18 mA cm^{-2}) is comparable with that (15–19 mA cm^{-2}) for solar cells based on PC$_{71}$BM/PTB7-Th.[9,10] However, the bottleneck is the low FF values of devices (<0.6), yet indicating the potential for further improvement. Further increase in DPE concentration to 10% deteriorates J_{sc}, V_{oc}, and FF values, thus PCE (6.70%). The J_{sc} values calculated from EQE of encapsulated TPB:PTB7-Th devices without/with 8% DPE as additive match well with J_{sc} values measured in encapsulated solar cell devices in <5% deviation. The TPB:PTB7-Th devices showed broad EQE spectra from 300 to 800 nm, in which the maximum values approach 75%. The spectral shape of EQE curves is similar to the absorption spectrum of blend films. To fulfill the potential of TPB based solar cells, further device optimization is in progress.

DFT Calculation, Electronic, and Optical Properties. To answer the question of why TPB exhibits high PCE values in OPV devices, the frontier molecular orbitals and the geometry of TPB were calculated based on the density functional theory with Gaussian package B3LYP/6-31g(d). In order to facilitate the calculation, one of the two alkyl chains in the PDI, far away from substitution position, was replaced with a methyl group. The resulting molecular geometry is shown in Figure 2a, and the LUMO and HOMO orbitals are presented in the Figure S2. It is clear that the HOMO electron density localizes at BDT-Th core, while the LUMO orbital localizes at PDI unit, suggesting a significant charge polarization in the exited state.

The optimized molecular geometry showed the dihedral angle between two PDIs and BDT is 58.9° and 50.2°, respectively, and a twist angle of 9° between the two PDI units connected with

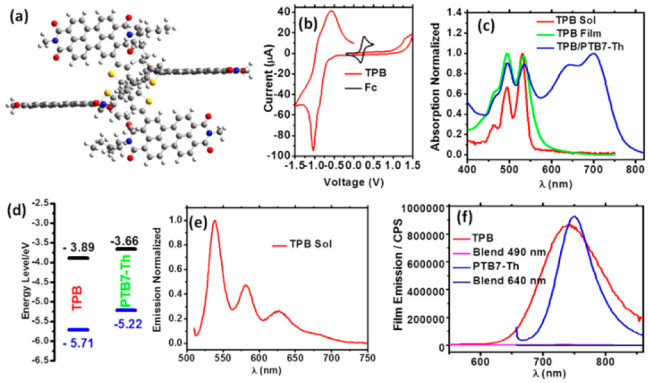

Figure 2. (a) Side view of calculated geometries of TPB. (b) Cyclic voltammograms of TPB film with Fc/Fc$^+$ as the reference. (c) Absorption spectra of TPB solution and film and blend film of TPB:PTB7-Th. (d) Schematic energy level of TPB and PTB7-Th. (e) Emission spectra of (e) TPB solution in chlorobenzene (10^{-7} M) and (f) TPB and PTB7-Th films and TPB:PTB7-Th blend film.

BDT. The dihedral angles between thiophene and BDT and thiophene and PDI are 50°, 50°, 55°, 55°, respectively, which lead to two parallel PDI units. The two PDI units connected through thiophene are nearly perpendicular to the plane of two PDIs connected through BDT. Therefore, the PDI moieties are still partially conjugated with the BDT-Th core. It can be envisioned that when a donor polymer chain interacts with a TPB molecule, only one of the four PDI units can have optimized π–π interaction due to steric effect, shown in Figure S4. Photoinduced charge transfer occurs from PTB7-Th to one of the PDI units; the electron can further find a pathway to be transmitted to other PDI units that is farther away from the donor polymer chain so that electron–hole binding energy between donor polymer and acceptor can be reduced due to longer distance.

As shown in Figure 2C, the UV–Vis absorption of TPB solution in chlorobenzene (10^{-7} M) exhibits three vibronic peaks between 450 and 550 nm with a maximum extinction coefficient of 2.33×10^{-5} M^{-1} cm^{-1} at 530 nm. The maximum absorption of TPB film appears at 575 nm, red-shifted by 24 nm from that in solution, which might reflect the extension of conjugation in solid state due to forced planarity caused by intermolecular interaction of TPB in the film. In contrast to the solution spectra, in which the strongest absorption peak is the 0–0 (I^{00}) transition, the strongest absorption peak in film is 0–1 (I^{01}) peak. The red-shifted maximum absorption and the strongest 0–1 (I^{01}) absorption peak of the film might suggest the intermolecular π–π stacking of TPB in the solid state.[8] The film absorption range (450–580 nm) of TPB complements to that of PTB7-Th (550–770 nm) and favors solar energy harvesting.

The LUMO and HOMO energy levels of TPB were determined to be −3.89 and −5.71 eV, respectively, (Figure 2b) with cyclic voltammetry studies using ferrocene (−4.8 eV) as standard reference; both of which match with the LUMO and HOMO of PTB7-Th with enough energy offset for both electron and hole transfer to each other (Figure 3d). It is worth noting that the HOMO energy difference between PTB7-Th and TPB is 0.49 eV, much smaller than that between PTB7-Th and PC$_{71}$BM (0.89 eV). Thus, holes generated in TPB can be more effectively extracted by PTB7-Th.[9]

The emission spectra of TPB in dilute chlorobenzene (10^{-7} M) are similar to those of PDI, with very limited emission quantum yield (QY) too weak to calculate, which is consistent

DOI: 10.1021/jacs.6b03562
J. Am. Chem. Soc. 2016, 138, 7248–7251

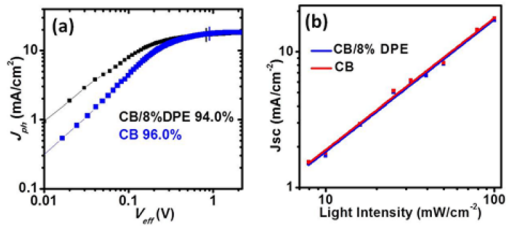

Figure 3. (a) Photocurrent density (J_{ph}) versus effective voltage (V_{eff}) characteristics of the two devices. (b) Short current density (J_{sc}) versus the light density of the two devices.

with the significant polarization in the excited state as shown by the DFT calculation. There is no significant change in absorption spectra of TPB in TPB/PTB7-Th blend films (Figure 2c) from that of pure TPB. The most relevant observation is that both TPB and PTB7-Th photoluminescence (PL) are almost completely quenched when they are excited at either 490 or 640 nm, indicating an efficient charge separation following excitation of either donor or acceptor.

This point is further reinforced by measurements of the charge dissociation probability $P(E, T)$. The $P(E, T)$ is defined as J_{ph}/J_{sat}; J_{ph} is defined by $J_L - J_D$ (J_L and J_D are light and dark current densities); J_{sat} is where the J_{ph} reaches its saturation at high reverse voltage, which means all the photogenerated exitons are dissociated to free charge carriers and collected by the electrodes. The plot of photo current density against the effective voltage V_{eff} (defined by $V_0 - V$, V_0 is voltage where $J_{ph} = 0$) in logarithmic scale allows the calculation of $P(E, T)$ under J_{sc} condition, yielding 96% and 94% for the as-deposited blend film and the blend film with 8% DPE as the additive, respectively (Figure 3a). The high and similar $P(E, T)$ values indicate the efficient exciton dissociation occurs at interfaces between TPB and PTB7-Th. The $P(E, T)$ values for the blend film with 8% DPE under 0−0.7 V work condition are higher than that for blend film without DPE, which is consistent with the FF improvement after adding 8% DPE. The measurement of the J_{sc} as a function of illumination intensity in logarithmic scale reveals insight into the recombination kinetics. If the slope of the curve reaches 1, then it implies weak bimolecular recombination, and the free carriers can be swept out and collected by the electrodes efficiently. In Figure 3b, the linear scaling of photocurrent to light intensity was observed for both devices with the same exponential factors of 0.97, indicating that the bimolecular recombination in the two devices is both very weak.

Active Layer Characterization. An intriguing observation is that the electron and hole mobility of the devices are very low, as measured by using the space-charge-limited current (SCLC) method with device structure of ITO/ZnO/TPB:PTB7-Th/Ca/Al for electrons and ITO/PEDOT:PSS/TPB:PTB7-Th/MoO_3/Ag for holes. The device without DPE additive gives electron and hole mobility of 4.13×10^{-6} and 6.65×10^{-6} cm^2 V^{-1} s^{-1}, respectively. After adding 8% DPE as the additive, the electron and hole mobility increases to 6.10×10^{-6} and 1.08×10^{-5} cm^2 V^{-1} s^{-1}, consistent with the observed FF increase from 0.47 to 0.58. The relatively low electron mobility is in agreement with the amorphous nature of TPB film (see Figure S6, the GIWAXS data), which is the reason for low FF value for TPB-based OPV devices, indicating further research direction.

Changes in PCE and mobility values imply changes in blend film morphology/topography. Since both donor and acceptor materials exhibit minimal contrast in atomic composition, transmission electron microscopy (TEM) results are not informative in phase separation (Figure 4). As shown in Figure 4c,d, the morphology of blend films spin-cast from chlorobenzene with and without 8% DPE shows fibrous features with fine and similar domain sizes, suggesting the minimal impact of DPE additive on the blend film morphology. However, it can be ascertained that the fibrous film morphology with fine domain size is beneficial to achieving the high J_{sc} values. However, atomic force microscopy (AFM) images indicated that the 8% DPE additive increases the root-mean-square (RMS) roughness of the blend film surface from 0.5 to 0.9 nm (Figure 4a,b). The higher RMS roughness of surface increases the contact area between the active layer and interfacial electrode, thus enhancing charge collection.[11]

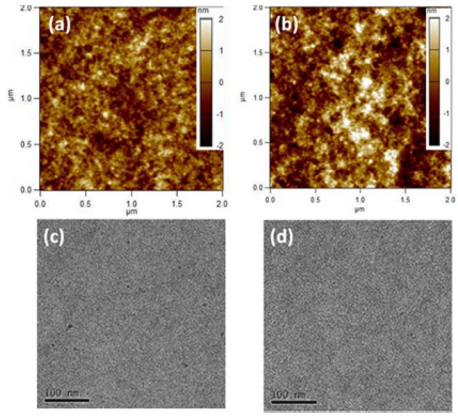

Figure 4. AFM of TPB/PTB7-Th films (a) without additive and (b) 8% DPE as additive. TEM images of the TPB/PTB7-Th films (c) without additive and (d) with 8% DPE as additive.

In summary, a new electron acceptor based on covalently bound clusters of alpha-substituted PDI was synthesized and exhibits promising potential for applications in OPV devices. The OPV device performance can be enhanced by using a small amount of DPE as cosolvent, which is accompanied by the improvement of hole/electron mobility. TPB-based devices also show the highest J_{sc} >18 mA/cm^2, which is comparable with that of $PC_{71}BM$/PTB7-Th based solar cells. DFT calculation shows that four PDIs in the TPB molecular form a cross-like molecular geometry, while they are still partially conjugated with the BDT-Th core. The effective PL quenching and charge dissociation probability measurements both demonstrate the efficient charge separation. The internal polarization is also important since EQE data showed significant contribution of charge generation from PTB within spectral range between 300 and 550 nm.

■ ASSOCIATED CONTENT

Supporting Information

The Supporting Information is available free of charge on the ACS Publications website at DOI: 10.1021/jacs.6b03562.

Synthesis, PL spectra, theoretical calculation, 2D-GIWAXS, and device fabrication and characterization. (PDF)

■ AUTHOR INFORMATION

Corresponding Author

*lupingyu@uchicago.edu

DOI: 10.1021/jacs.6b03562
J. Am. Chem. Soc. 2016, 138, 7248−7251

Author Contributions

‖These authors contributed equally.

Notes

The authors declare no competing financial interest.

■ ACKNOWLEDGMENTS

This work was supported by U.S. National Science Foundation grant (NSF DMR-1263006) and NSF MRSEC program at the University of Chicago (DMR-0213745), DOE via the ANSER Center, an Energy Frontier Research Center funded by the U.S. Department of Energy, Office of Science, Office of Basic Energy Sciences, under award no. DE-SC0001059 and NIST via CHIMAD program. Use of the Advanced Photon Source (APS) at Argonne National Laboratory was supported by the U.S. Department of Energy, Office of Science, Office of Basic Energy Sciences, under contract no. DE-AC02-06CH11357.

■ REFERENCES

(1) Eftaiha, A. a. F.; Sun, J.-P.; Hill, I. G.; Welch, G. C. *J. Mater. Chem. A* **2014**, *2*, 1201.

(2) (a) Sonar, P.; Lim, J. P. F.; Chan, K. L. *Energy Environ. Sci.* **2011**, *4*, 1558. (b) Li, C.; Wonneberger, H. *Adv. Mater.* **2012**, *24*, 613.

(3) (a) Sun, D.; Meng, D.; Cai, Y.; Fan, B.; Li, Y.; Jiang, W.; Huo, L.; Sun, Y.; Wang, Z. *J. Am. Chem. Soc.* **2015**, *137*, 11156. (b) Li, H.; Hwang, Y.-J.; Courtright, B. A. E.; Eberle, F. N.; Subramaniyan, S.; Jenekhe, S. A. *Adv. Mater.* **2015**, *27*, 3266. (c) Zhong, Y.; Trinh, M. T.; Chen, R.; Purdum, G. E.; Khlyabich, P. P.; Sezen, M.; Oh, S.; Zhu, H.; Fowler, B.; Zhang, B.; Wang, W.; Nam, C.-Y.; Sfeir, M. Y.; Black, C. T.; Steigerwald, M. L.; Loo, Y.-L.; Ng, F.; Zhu, X. Y.; Nuckolls, C. *Nat. Commun.* **2015**, *6*, 8242. (d) Lin, Y.; He, Q.; Zhao, F.; Huo, L.; Mai, J.; Lu, X.; Su, C.-J.; Li, T.; Wang, J.; Zhu, J.; Sun, Y.; Wang, C.; Zhan, X. *J. Am. Chem. Soc.* **2016**, *138*, 2973. (e) Hwang, Y. J.; Li, H. Y.; Courtright, B. A. E.; Subramaniyan, S.; Jenekhe, S. A. *Adv. Mater.* **2016**, *28*, 124. (f) Holliday, S.; Ashraf, R. S.; Nielsen, C. B.; Kirkus, M.; Rohr, J. A.; Tan, C.-H.; Collado-Fregoso, E.; Knall, A.-C.; Durrant, J. R.; Nelson, J.; McCulloch, I. *J. Am. Chem. Soc.* **2015**, *137*, 898. (g) Yan, Q.; Zhou, Y.; Zheng, Y.-Q.; Pei, J.; Zhao, D. *Chemical Science* **2013**, *4*, 4389. (h) Lin, Y.; Wang, J.; Dai, S.; Li, Y.; Zhu, D.; Zhan, X. *Adv. Energy. Mater.* **2014**, *4*, 201300626. (i) Lin, Y.; Wang, Y.; Wang, J.; Hou, J.; Li, Y.; Zhu, D.; Zhan, X. *Adv. Mater.* **2014**, *26*, 5137.

(4) Kwon, O. K.; Park, J.-H.; Kim, D. W.; Park, S. K.; Park, S. Y. *Adv. Mater.* **2015**, *27*, 1951.

(5) (a) Yang, Y.; Zhang, G.; Yu, C.; He, C.; Wang, J.; Chen, X.; Yao, J.; Liu, Z.; Zhang, D. *Chem. Commun.* **2014**, *50*, 9939. (b) Lin, Y.; Zhang, Z.-G.; Bai, H.; Wang, J.; Yao, Y.; Li, Y.; Zhu, D.; Zhan, X. *Energy Environ. Sci.* **2015**, *8*, 610. (c) Zhao, J.; Li, Y.; Lin, H.; Liu, Y.; Jiang, K.; Mu, C.; Ma, T.; Lai, J. Y. L.; Hu, H.; Yu, D.; Yan, H. *Energy Environ. Sci.* **2015**, *8*, 520.

(6) Zang, Y.; Li, C.-Z.; Chueh, C.-C.; Williams, S. T.; Jiang, W.; Wang, Z.-H.; Yu, J.-S.; Jen, A. K. Y. *Adv. Mater.* **2014**, *26*, 5708.

(7) (a) Lin, Y.; Wang, J.; Zhang, Z.-G.; Bai, H.; Li, Y.; Zhu, D.; Zhan, X. *Adv. Mater.* **2015**, *27*, 1170. (b) Liu, Y.; Mu, C.; Jiang, K.; Zhao, J.; Li, Y.; Zhang, L.; Li, Z.; Lai, J. Y. L.; Hu, H.; Ma, T.; Hu, R.; Yu, D.; Huang, X.; Tang, B. Z.; Yan, H. *Adv. Mater.* **2015**, *27*, 1015. (c) Lee, J.; Singh, R.; Sin, D. H.; Kim, H. G.; Song, K. C.; Cho, K. *Adv. Mater.* **2016**, *28*, 69.

(8) (a) Zhao, D.; Wu, Q.; Cai, Z.; Zheng, T.; Chen, W.; Lu, J.; Yu, L. *Chem. Mater.* **2016**, *28*, 1139. (b) Zhang, J.; Singh, S.; Hwang, D. K.; Barlow, S.; Kippelen, B.; Marder, S. R. *J. Mater. Chem. C* **2013**, *1*, 5093.

(9) He, Z.; Xiao, B.; Liu, F.; Wu, H.; Yang, Y.; Xiao, S.; Wang, C.; Russell, T. P.; Cao, Y. *Nat. Photonics* **2015**, *9*, 174.

(10) Lu, L.; Xu, T.; Chen, W.; Landry, E. S.; Yui, L. *Nat. Photonics* **2014**, *8*, 716.

(11) (a) Park, H.-Y.; Lim, D.; Kim, K.-D.; Jang, S.-Y. *J. Mater. Chem. A* **2013**, *1*, 6327. (b) Sekine, N.; Chou, C.-H.; Kwan, W. L.; Yang, Y. *Org. Electron.* **2009**, *10*, 1473. (c) Gu, C.; Zhang, Z.; Sun, S.; Pan, Y.; Zhong, C.; Lv, Y.; Li, M.; Ariga, K.; Huang, F.; Ma, Y. *Adv. Mater.* **2012**, *24*, 5727.

DOI: 10.1021/jacs.6b03562
J. Am. Chem. Soc. 2016, 138, 7248−7251